Valeri V. Mossine*, Steven P. Kelley and Thomas P. Mawhinney

Crystal structure of (*E*)-3-methoxy-*N*′-(1-(pyridin-2-yl)ethylidene)benzohydrazide, $C_{15}H_{15}N_3O_2$

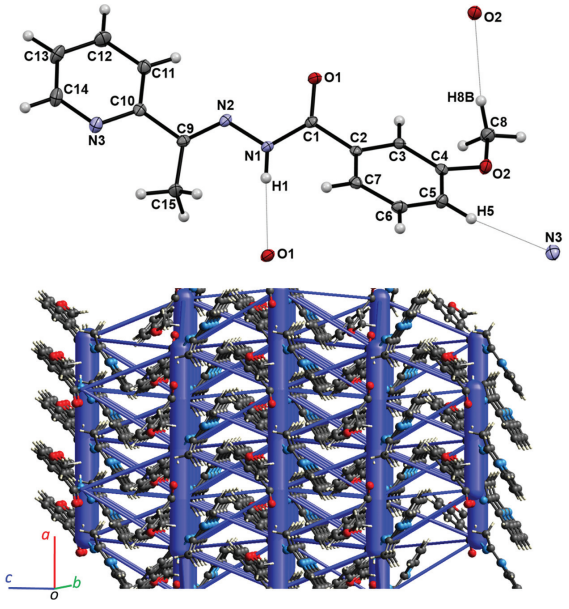

https://doi.org/10.1515/ncrs-2020-0097
Received February 18, 2020; accepted March 10, 2020; available online March 25, 2020

Abstract

$C_{15}H_{15}N_3O_2$, orthorhombic, $Pca2_1$ (no. 29), $a = 7.9831(2)$ Å, $b = 10.6486(3)$ Å, $c = 15.7222(4)$ Å, $V = 1336.53(6)$ Å^3, $Z = 4$, $R_{gt}(F) = 0.0340$, $wR_{ref}(F^2) = 0.0799$, $T = 100$ K.

CCDC no.: 1989321

Table 1 contains crystallographic data and Table 2 contains the list of the atoms including atomic coordinates and displacement parameters.

***Corresponding author: Valeri V. Mossine,** Department of Biochemistry, University of Missouri, Columbia, MO 65211, USA, Tel.: 1-573-882-2608, Fax: 1-573-884-4631, e-mail: mossinev@missouri.edu. https://orcid.org/0000-0003-3000-5673
Steven P. Kelley: Department of Chemistry, University of Missouri, Columbia, MO 65211, USA
Thomas P. Mawhinney: Department of Biochemistry, University of Missouri, Columbia, MO 65211, USA

Table 1: Data collection and handling.

Crystal:	Colourless prism
Size:	0.28 × 0.22 × 0.09 mm
Wavelength:	Mo $K\alpha$ radiation (0.71073 Å)
μ:	0.09 mm^{-1}
Diffractometer, scan mode:	Bruker APEX-II, φ and ω
θ_{max}, completeness:	29.7°, >99%
$N(hkl)_{measured}$, $N(hkl)_{unique}$, R_{int}:	34842, 3790, 0.049
Criterion for I_{obs}, $N(hkl)_{gt}$:	$I_{obs} > 2\ \sigma(I_{obs})$, 3385
$N(param)_{refined}$:	186
Programs:	Bruker [1], SHELX [2, 3], Olex2 [4], Crystal Explorer [5], Mercury [6]

Source of material

To a suspension of 831 mg (5 mmoles) *m*-anisic hydrazide in 15 mL 90% aqueous EtOH were added 606 mg (561 µL, 5 mmoles) 2-acetylpyridine, and the reaction mixture was stirred for 6 h at 70 °C. The resulting clear solution was brought to 4 °C and left for 2 days to deposit crystals as colorless prisms.

Experimental details

The hydrazide H1 atom was located in difference-Fourier maps while all other hydrogen atoms were initially placed in calculated positions. Thermal parameters were constrained to ride on the carrier atoms (U_{iso}(methine H) = 1.2U_{eq} and U_{iso}(methyl H) = 1.5U_{eq}). Due to a high uncertainty on the Flack parameter (0.279), no attempt to model inversion twinning was made.

Comment

One particular interest to hydrazide-hydrazones, a versatile group of organic molecules, stems from their high affinity to iron, which makes these structures potential antimicrobial [7, 8], anticancer [9], or neuroprotective [10] agents. As a part of our search for inhibitors of cytotoxic virulence factors from drug-resistant bacteria [11], we have prepared the title compound, a structural analogue of a series of hydrazide-hydrazones that are pharmacologically active in vivo.

The title compound crystallizes in the orthorhombic $Pca2_1$ space group, with four equivalent molecules per unit cell. The asymmetric unit of the title structure contains one molecule of 2-acetylpyridine *m*-anisoyl

Table 2: Fractional atomic coordinates and isotropic or equivalent isotropic displacement parameters (Å^2).

Atom	*x*	*y*	*z*	U_{iso}*/U_{eq}
O1	0.65856(15)	0.64702(11)	0.53292(9)	0.0163(3)
O2	1.13033(16)	0.94314(11)	0.64302(8)	0.0172(3)
N1	0.81973(18)	0.47369(13)	0.50812(9)	0.0123(3)
N2	0.69467(17)	0.42449(13)	0.45744(9)	0.0122(3)
N3	0.5631(2)	0.13527(14)	0.37099(10)	0.0164(3)
C1	0.7893(2)	0.58803(16)	0.54361(10)	0.0115(3)
C2	0.9256(2)	0.63898(15)	0.59947(11)	0.0114(3)
C3	0.9580(2)	0.76818(15)	0.59386(11)	0.0120(3)
C4	1.0831(2)	0.81951(16)	0.64451(11)	0.0132(3)
C5	1.1709(2)	0.74460(17)	0.70209(11)	0.0156(3)
C6	1.1347(2)	0.61830(17)	0.70823(12)	0.0157(3)
C7	1.0126(2)	0.56340(15)	0.65637(10)	0.0134(3)
C8	1.0461(2)	1.02502(16)	0.58479(12)	0.0190(4)
C9	0.7113(2)	0.31023(15)	0.43228(11)	0.0123(3)
C10	0.5685(2)	0.26067(16)	0.38103(10)	0.0125(3)
C11	0.4476(2)	0.34046(17)	0.34663(11)	0.0169(4)
C12	0.3153(3)	0.28838(19)	0.30172(13)	0.0231(4)
C13	0.3086(3)	0.15935(19)	0.29134(14)	0.0233(4)
C14	0.4345(3)	0.08763(17)	0.32668(13)	0.0198(4)
C15	0.8537(2)	0.22489(17)	0.45435(14)	0.0225(4)
H1	0.916(3)	0.438(2)	0.5112(14)	0.015*
H3	0.895440	0.819679	0.556100	0.014*
H5	1.255451	0.780516	0.736965	0.019*
H6	1.193383	0.567925	0.748208	0.019*
H7	0.989501	0.476039	0.660006	0.016*
H8A	1.093279	1.109719	0.589322	0.029*
H8B	0.926414	1.027556	0.598559	0.029*
H8C	1.060933	0.993830	0.526631	0.029*
H11	0.455732	0.428818	0.353844	0.020*
H12	0.230380	0.340505	0.278372	0.028*
H13	0.219625	0.121204	0.260656	0.028*
H14	0.429805	−0.000820	0.319174	0.024*
H15A	0.877896	0.231453	0.515294	0.034*
H15B	0.953112	0.249219	0.421713	0.034*
H15C	0.823311	0.138099	0.440495	0.034*

hydrazone (2APymAH), shown in the upper part of the figure. The valence bond lengths and angles are in the expected ranges. The major portion of the molecule is approximately flat: all but three atoms, O1, H8C, and H15B, are located within 1 Å of the mean molecular plane. The pyridyl and the anisyl ring planes are at 10.0° and 13.3° to the molecular plane, respectively. The conventional hydrogen bonding in crystal structure of 2APymAH is limited to only one intermolecular heteroatom contact (N1···O1 = 3.020(2) Å, H1···O1 = 2.17(2) Å, N1—H1···O1 = 174(2)°) shown in the upper part of the figure. In the crystal, infinite chains of the H-bonds propagate in the [100] direction. In addition, two short intermolecular contacts of the C—H···O/N type, which satisfy to the directionality condition (angle C—H···O/N > 120°) and which are shown in the figure as dotted lines, may contribute to the stability of the molecular packing in the 2APymAH crystal, as well. The crystal structure lacks any strong π-π stacking interactions, with the shortest contact between the pirydyl (ring 1) and the anisyl (ring 2) rings Cg1···Cg2′ = 5.1198(11) Å (′ = −1/2 + *x*, 1 − *y*, *z*). In addition, a short C5—H5···Cg1″ (″ = 2 − *x*, 1 − *y*, 1/2 + *z*) contact is present in the crystal structure, as well.

To account for all interactions involved in the build-up of the crystal structure, we have performed DFT calculations, at the B3LYP/6-31G(d,p) theory level [5, 12], of the electrostatic, dispersion, polarization, and repulsion energies in the 2APymAH crystal structure. According to the calculations, the interactions from hydrogen-bonded pairs of molecules contributed about 50% to the lattice energy, with the dispersion energy providing most for the attractive forces between neighbouring molecules of 2APymAH (i.e. $E_{elstat} = -54$ kJ/mol, $E_{disp} = -75.2$ kJ/mol for $x + 1/2$, $-y$, z). The spatial distribution of the energetically most significant interactions is illustrated in the lower part of the figure, showing the interactions energy framework as blue cylinders penetrating the crystal lattice of 2APymAH. The cylinders connect centroids of the interacting molecules, and their diameters are proportional to the total energies of the interactions, with the 8 kJ/mol cutoff, for clarity. The most extensive intermolecular interactions occur in the H-bonding direction parallel to [100]. To estimate the lattice energy, all total energies of unique pairwise interactions between molecules were summed up, thus yielding $E_{lattice} = -164$ kJ/mol for the 2APymAH crystal.

Acknowledgements: We gratefully acknowledge financial support by the University of Missouri Agriculture Experiment Station Chemical Laboratories and by the National Institute of Food and Agriculture (grant MO-HABC0002).

References

1. Bruker Axs Inc., Apex3 v. 2016.9-0 and SAINT v. 8.37A. Madison, WI, USA (2016).
2. Sheldrick, G. M.: A short history of SHELX. Acta Crystallogr. **A64** (2008) 112–122.
3. Sheldrick, G. M.: Crystal structure refinement with SHELXL. Acta Crystallogr. **C71** (2015) 3–8.
4. Dolomanov, O. V.; Bourhis, L. J.; Gildea, R. J.; Howard, J. A. K.; Puschmann, H.: OLEX2: a complete structure solution, refinement and analysis program. J. Appl. Crystallogr. **42** (2009) 339–341.
5. MacKenzie, C. F.; Spackman, P. R.; Jayatilaka, D.; Spackman, M. A.: CrystalExplorer model energies and energy frameworks: extension to metal coordination compounds, organic salts, solvates and open-shell systems. IUCrJ **4** (2017) 575–587.
6. Macrae, C. F.; Bruno, I. J.; Chisholm, J. A.; Edgington, P. R.; McCabe, P.; Pidcock, E.; Rodriguez-Monge, L.; Taylor, R.; van

de Streek, J.; Wood, P. A.: Mercury CSD 2.0 – new features for the visualization and investigation of crystal structures. J. Appl. Crystallogr. **41** (2008) 466–470.
7. Narang, R.; Narasimhan, B.; Sharma, S.: A review on biological activities and chemical synthesis of hydrazide derivatives. Curr. Med. Chem. **19** (2012) 569–612.
8. Rzhepishevska, O.; Hakobyan, S.; Ekstrand-Hammarstroem, B.; Nygren, Y.; Karlsson, T.; Bucht, A.; Elofsson, M.; Boily, J.-F.; Ramstedt, M.: The gallium(III)-salicylidene acylhydrazide complex shows synergistic anti-biofilm effect and inhibits toxin production by *Pseudomonas aeruginosa*. J. Inorg. Biochem. **138** (2014) 1–8.
9. Lovejoy, D. B.; Richardson, D. R.: Iron chelators as anti-neoplastic agents: Current developments and promise of the PIH class of chelators. Curr. Med. Chem. **10** (2003) 1035–1049.
10. Richardson, D. R.: Novel chelators for central nervous system disorders that involve alterations in the metabolism of iron and other metal ions. Ann. N. Y. Acad. Sci. **1012** (2004) 326–341.
11. Mossine, V. V.; Waters, J. K.; Chance, D. L.; Mawhinney, T. P.: Transient proteotoxicity of bacterial virulence factor pyocyanin in renal tubular epithelial cells induces ER-related vacuolation and can be efficiently modulated by iron chelators. Toxicol. Sci. **154** (2016) 403–415.
12. Thomas, S. P.; Spackman, P. R.; Jayatilaka, D.; Spackman, M. A.: Accurate lattice energies for molecular crystals from experimental crystal structures. J. Chem. Theory Comput. **14** (2018) 1614–1623.